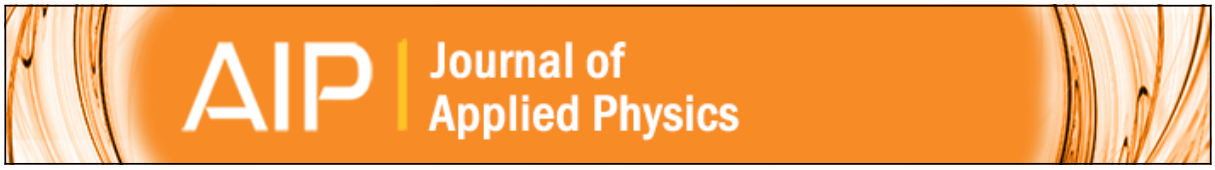

Use of hydrogenation in the study of the properties of amorphous germanium tin alloys

I. Chambouleyron and F. C. Marques

Citation: Journal of Applied Physics **65**, 1591 (1989); doi: 10.1063/1.342950

View online: http://dx.doi.org/10.1063/1.342950

View Table of Contents: http://scitation.aip.org/content/aip/journal/jap/65/4?ver=pdfcov

Published by the AIP Publishing

Use of hydrogenation in the study of the properties of amorphous germanium tin alloys

I. Chambouleyron and F. C. Marques
Instituto de Fisica, Universidade Estadual de Campinas, P. O. Box 6165, Campinas, S. P., Brazil

(Received 20 June 1988; accepted for publication 19 October 1988)

A study of the macroscopic properties of *a*-Ge:Sn and *a*-Ge:Sn:H films is presented. The samples were prepared by the rf sputtering method on substrates held at 180 °C. Their composition and structure were characterized, and the transport and optical properties were studied. The role and influence of hydrogen on the general properties of the alloys have been established.

I. INTRODUCTION

The two most studied classes of amorphous semiconductors are chalcogenide glasses and tetrahedrally bonded alloys. Only the latter can be prepared as electronic materials in the sense that their electrical conductivity can be modulated by appropriate chemical doping.[1] It is by now well established that these characteristics are a direct consequence of the role of hydrogen as a dangling bond passivating agent in the network. Today *a*-Si:H is an electronic semiconductor of controllable quality. On the basis of the present knowledge of the physics and chemistry of *a*-Si:H films, remarkable progress has been made in device manufacturing, i.e., high efficiency *p-i-n* solar cells, thin-film transistors, electrophotography, and imaging devices.[2]

The study of *a*-Ge:H films has been relegated as compared to *a*-Si:H, mainly because the material obtained by different deposition methods does not have good electronic properties. The reasons for this deficiency are not clear yet. Recent advances have been reported on hydrogenated and fluorinated *a*-Ge.[3]

The need of cheap and efficient materials for the photovoltaic conversion of solar energy, and the possibility of manufacturing multiple junction amorphous solar cells, lead many research groups to investigate new compound amorphous semiconductors. The possibility of tailoring the optoelectronic properties of such alloys by varying their composition considerably widens the existing application spectrum. Today, most of the research efforts are directed towards the understanding and mastering of the properties of *a*-Si:Ge:H alloys. On the narrow-band-gap side, some work has been done on *a*-Si:Sn:H, where it has been found that its electronic properties degrade very rapidly as the tin content in the alloy increases.[4]

The *a*-Ge:Sn system was first prepared by Temkin, Connell, and Paul[5] and the properties of unhydrogenated alloys deposited at − 10 °C were reported. In the present paper we are concerned with the properties of hydrogenated and unhydrogenated amorphous Ge-Sn films deposited at higher temperatures (180 °C). The general properties of these films, as well as the influence of hydrogen atoms on the optical and transport properties of the alloys, are presented and discussed for the first time.

II. EXPERIMENT

A. Material preparation

Amorphous Ge and $Ge_{1-x}Sn_x$, as well as *a*-Ge:H and *a*-$Ge_{1-x}Sn_x$:H films, were deposited by the rf sputtering method in a Leybold Heraus Z-400 apparatus. The target was a 2-in.-diam, 1/4-in.- thick, 99.999% pure Ge disk upon which small pieces of 99.999% Sn were placed in an approximately random way to prepare alloy films. The system was dry pumped, prior to deposition, to a base pressure of 10^{-6} mbar for 1 h. The argon gas was of 99.9995-at. % nominal purity. All samples were prepared under identical deposition conditions, the only variable being the Sn target coverage. A series of five samples corresponds to unhydrogenated films, and another series of five to hydrogenated material. The tin content of the samples varied between 0 and around 30 at. %. The substrates, quartz, near-intrinsic crystalline silicon, and Corning 7959 glass, were ultrasonically precleaned and kept at 180 °C during deposition. Typical sample thickness was 1 μm. The target was plasma etched for several minutes before starting each run. The total pressure was 0.015 mbar in all cases. For hydrogenated samples the H_2 partial pressure was adjusted prior to deposition. During the discharge the hydrogen flow was kept constant. The rf power was adjusted in each series in order to give a deposition rate of approximately 1 Å/s. As the sputtering yield is higher for Sn than for Ge, a constant deposition rate for all samples implies a varying rf power, which has to be decreased as the metal coverage of the Ge target increases. One of the consequences of the smaller rf power fed into the plasma is a poorer hydrogenation of the metal-rich films.

B. Measurements

After deposition the structural properties were investigated by x-ray diffraction in a PW 1140 Philips generator (Cu$K\alpha$ line) coupled to a diffractometer at a scan speed of 0.5 deg/min. All the samples proved to be x-ray amorphous. Nevertheless, the hydrogenated samples having larger tin contents showed some of the characteristic diffraction peaks of β-Sn, a clear indication of metallic segregation. In the case of the sample with the highest concentration of tin (27 at. %), the metal particles on the surface could be detected

 0021-8979/89/041591-07$02.40

by visual inspection. The topography and composition of unhydrogenated samples were determined by several methods. Topography images were obtained by secondary electron imaging and the composition by electron probe microanalysis using a scanning electron microscope CAMECA model Camebax. A beam energy of 15 keV was chosen in order to avoid interactions of the probe with the substrate. Under these conditions the probe penetration for pure Ge is of the order of 0.5 μm. These results were compared with those obtained from x-ray photoelectron spectroscopy performed in a McPherson 36 electron spectrometer for chemical analysis (ESCA), and also with sample composition obtained with Rutherford backscattering spectrometry (RBS) techniques. Finally, the composition and bonding configuration of unhydrogenated films were analyzed by conversion electrons Mössbauer spectroscopy (CEMS). The results of this specific study are given in Ref. 6.

The optical transmission of the samples was measured in the visible and infrared regions of the spectrum. In the 4000–25 000 wave-number range a Karl Zeiss DMR 21 spectrophotometer was used, while a Jasco A 202 infrared apparatus gave the transmission features in the 400–4000 wave-number range. The hydrogen content of the films was deduced from the integrated area under the absorption peak corresponding to the Ge-H wagging mode.[7]

Coplanar 10-mm-long aluminum strips 1 mm apart were evaporated on the samples. Excellent ohmic behavior was observed in the 10–100-V polarization range. Conductivity measurements were made using dc biases of 50 V, and 10 V for hydrogenated and unhydrogenated samples, respectively. The dark conductivity was measured in an evacuated chamber in the 120–400-K range. Photoconductivity measurements were made only at room temperature using a mercury-halogen lamp (ELH) and a radiation power density of 80 mW/cm^2.

III. RESULTS

A. Material composition

An overview of the estimated and measured composition of the samples is given in Table I. The tin concentrations estimated from the sputtering yield of each element and the area covered by metallic Sn are in all cases inferior to the content measured, either by ESCA or RBS. The discrepancy might have its origin in a wrong estimate of the sputtered area. The uncertainity in the composition measured with ESCA is of nearly 35%. RBS spectra of unhydrogenated samples deposited onto glass substrates indicate that there is no segregation, neither in the outermost surface nor in the interior of the film.[6] These considerations lead us to believe that the composition given by RBS is nearer to the true material composition. Tin concentration values of a couple of samples were also determined with electron probe microanalysis. The resulting values ranged between those given by ESCA and RBS measurements. It is important to stress here that these material composition studies were only made in unhydrogenated samples. Hydrogenated samples are assumed to have the same tin to germanium relative content. In other words, the Ge-Sn alloy behaves as a single component of the new hydrogenated alloy. Therefore, the composition of hydrogenated samples should be thought of as $(Ge_{1-x}Sn_x)_{1-y}:H_y$.

A few comments are worthwhile in referring to metallic segregation. It has been observed that the tendency of the material to segregate metallic tin strongly depends on three deposition parameters: the substrate temperature, the coverage of the target, and the hydrogen partial pressure during the discharge. The increase of any one of the three increases the segregation tendency. Evidently, the tendency is accentuated if more than one of the mentioned deposition parameters are increased simultaneously.

TABLE I. Deposition rate, thickness, and composition of the rf sputtered *a*-Ge:Sn and *a*-Ge:Sn:H samples.

Sample No.	Tin (at. %) a	Tin (at. %) ESCA	Tin (at. %) RBS	Hydrogen (at. %)	Dep. rate (Å/s)	Thick. (μm)
01	0	···	0	0	0.9	0.85
02	0	···	0	14	0.9	1.02
03	1	4	4	0	1.2	1.08
04	1	···	4	9	1.1	0.99
05	10	23	15	0	1.0	0.92
06	10	···	15	5	1.0	0.94
07	15	···	(21[b])	0	1.0	0.90
08	15	···	···	?	1.0	···
09	20	40	27	0	1.0	0.90
10	20	···	···	?	1.0	···

[a] Estimated from sputtering yield and target coverage.

[b] The composition of sample No. 07 (21-at.% tin) has been deduced from the metal coverage of the target and the RBS composition of sample Nos. 05 and 09.

B. Optical properties

Figure 1 shows a Tauc's law type plot of some of the samples listed in Table I. The extrapolated optical gaps are also indicated and listed in Table II. It is clear from the figure that the pseudogap of these amorphous alloys narrows as the tin concentration increases. It is also evident that hydrogen acts in an opposite way, i.e., it widens the pseudogap. Other effects of hydrogenation appear in Figs. 2 and 3. Figure 2 shows the infrared transmission of two identical samples, except their hydrogen content. Two main absorption peaks appear. They have been associated in the literature[7] to the

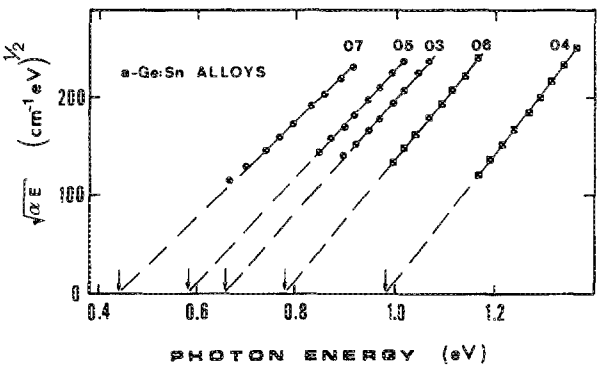

FIG. 1. Square root of the product of the absorption coefficient and the photon energy for some of the samples of Table I. The extrapolated optical band gaps are also indicated.

TABLE II. Optical and transport properties of the *a*-Ge. *a*-Ge:H, *a*-Ge:Sn, and *a*-Ge:Sn:H samples.

Sample No.	Forbidden band (eV)	Refractive index (at IR)	Activation energy (eV) (300–400 K)	Room-temp. conductivity $(\Omega\ \mathrm{cm})^{-1}$
01	0.70	4.38	...	5.7×10^{-3}
02	1.04	3.96	0.45	1.8×10^{-5}
03	0.66	4.43	...	1.7×10^{-2}
04	0.98	4.05	0.48	1.2×10^{-5}
05	0.58	4.73	...	5.6×10^{-2}
06	0.78	4.32	0.34	1.4×10^{-3}
07	0.44	5.0[a]	...	...
08	...	...	...	...
09	0.37	5.2[a]	...	3.0×10^{-1}
10	...	...	...	...

[a] Estimated.

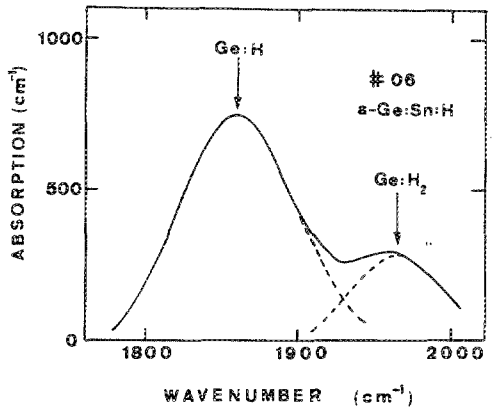

FIG. 3. Absorption coefficient vs photon energy of the stretching vibration of a hydrogenated Ge:Sn sample. The absorption band can be well fitted with two Gaussian curves corresponding to the Ge-H and Ge-H_2 vibrational modes. However, the absorption peak is slightly shifted towards lower energy.

stretching and the wagging vibrations of the Ge-H (1895 and 565 cm^{-1}) configurations, respectively. No specific absorption features related to Sn-H or to Sn-H_2 have been observed in any sample. Table I also indicates that as the tin content increases in the samples, the hydrogen content decreases. As already explained, this fact is certainly the consequence of keeping a constant deposition rate for all sample compositions, which in turn implies a smaller rf power in the plasma for Sn richer samples. A decreased rf power during deposition means a lower concentration of atomic hydrogen in the plasma and, consequently, a lower H content in the films. Figure 3 shows the form of the stretching absorption band. The dashed lines represent the best fit to experimental points given by a couple of Gaussian-type absorption bands. They are similar in shape and energy to the reported absorption bands of amorphous germanium.[7]

C. Transport properties

Figure 4 shows the effects of hydrogenation on the transport properties of amorphous germanium (samples No. 01 and No. 02). Remember that these *a*-Ge and *a*-Ge:H films were grown under conditions indentical to those used to prepare the Ge-Sn alloys. They are the reference samples in the present study. Figure 4 indicates, for both samples, the dark conductivity versus the inverse absolute temperature. Within our experimental measurement range *a*-Ge:H possesses an activated type conductivity. The improvement of the electronic properties of *a*-Ge by the use of hydrogen has been amply reported in the literature[8,9] and explained in terms of dangling bond passivation and network relaxation. The results of Fig. 4 confirm previous reports and will be useful for comparison purposes when studying similar effects in Ge-Sn alloys.

Figure 5 shows the dark conductivity versus the inverse absolute temperature of some samples of Table I. It becomes apparent from the figure that the presence of hydrogen during the deposition process greatly modifies the conduction mechanisms of the Ge-Sn layers, in a way similar to that observed in Fig. 4 for pure *a*-Ge. However, some significant differences appear in the values of the corresponding activation energies and in the general shape of the curves. As ex-

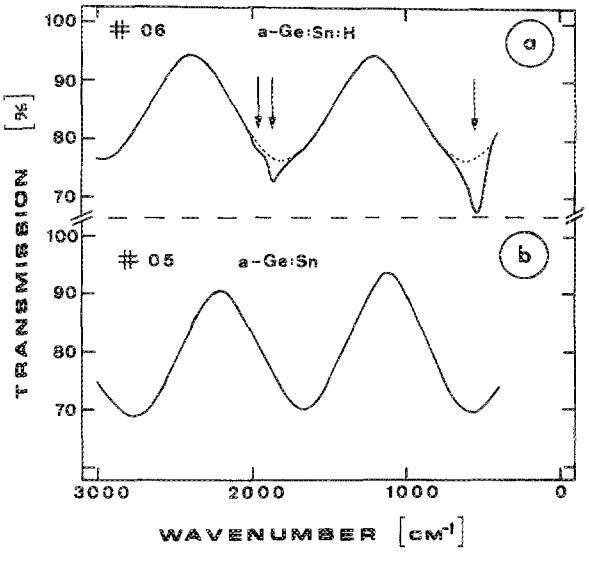

FIG. 2. Infrared transmission spectra of two *a*-Ge:Sn films. The absorption peaks appearing on the hydrogenated sample correspond to the stretching and wagging modes of the Ge-H and Ge-H_2 configuration.

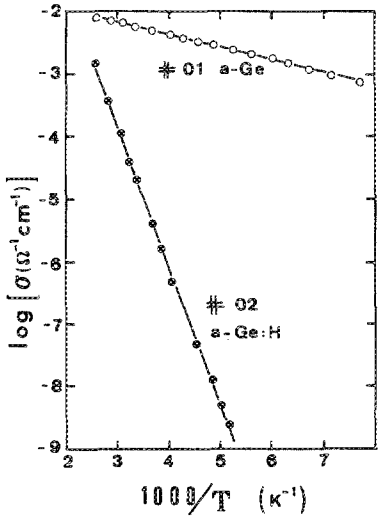

FIG. 4. Dark conductivity of *a*-Ge:H films as a function of inverse temperature. The presence of hydrogen in the reactor chamber changes the conductivity by orders of magnitude and the electronic conduction becomes an activated process.

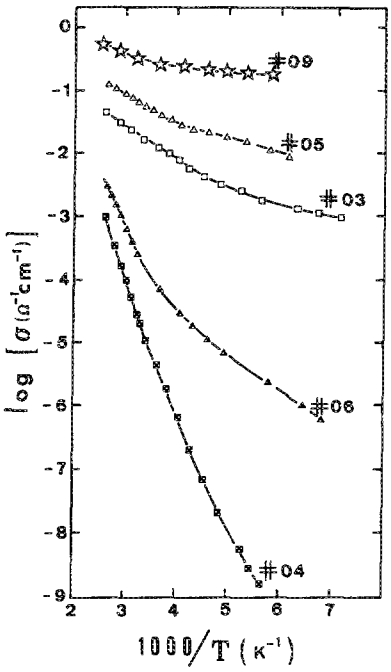

FIG. 5. Dark conductivity of *a*-Ge:Sn and *a*-Ge:Sn:H films as a function of inverse temperature. The beneficial effects of hydrogen in removing electronic states in the pseudogap can be clearly seen. The conduction process becomes activated but the activation energies and the temperature range of activated conduction depend on alloy composition.

pected, the activation energies become smaller as the band gap of the alloy decreases. Futhermore, the temperature range of activated conduction decreases and other conduction paths (not through extended states in the bands) appear to contribute up to higher temperatures. This behavior may be due to a combination of several causes. Among them we may cite the following: the decreasing H content in the samples as the tin content increases; an increased density of Ge defect centers due to network strains; or the appearance of new electronic states in the band gap. Unhydrogenated samples seem to have two different conductivity regions, the high-temperature one appearing to be of the activated type.

IV. DISCUSSION

A. Alloy composition and metallic segregation

Under equilibrium conditions the solubility of tin in germanium is very low.[10] However, rapid cooling methods allow preparation of supersaturated solutions of Sn in Ge. In this case Mössbauer spectroscopy confirms that the Sn atoms in the crystalline Ge lattice form sp^3 hybrid chemical bonds typical of Ge and α-Sn.[11] Temkin and Paul[12] studied the structural and optical properties of amorphous $Ge_{1-x}Sn_x$ films in the range $x \leqslant 0.5$. These authors showed that it was possible to prepare amorphous films containing higher tin content by the rf sputtering of pressed powder targets in argon, the substrates being held at -10 °C. Under these preparation conditions the amorphous films have a random tetrahedral bonding, the relative ratio of Ge—Sn bonds to Ge—Ge bonds (and to Sn—Sn bonds) being of around 2:1 in the $x = 0.5$ composition. In a recent work,[6] our group reported on the structure and composition of *a*-Ge:Sn unhydrogenated samples prepared at higher temperatures (180 °C) and cooled down at a slow rates (~ 2 °C/min). CEMS studies on samples having up to 27-at. % tin confirm the presence of ^{119m}Sn in amorphous germanium. The CEMS spectra could be perfectly fitted with just one singlet, the characteristics of which indicate that all Sn atoms appear to bond to four Ge atoms in a covalent tetrahedral configuration. In other words, no defect structures could be detected by Mössbauer spectroscopy around tin sites. These results established some new features concerning the bonding configuration of the alloys as compared to the results of Ref. 5.

In a complementary work[12] the group at Harvard studied the crystallization temperature (T_c) of alloyed samples containing varying amounts of tin. Their data may be fitted approximately by $T_c(\mathrm{K}) \sim 770(1-x)$, an empirical finding announcing that an upper limit of around 60-at. % tin exists for an amorphous Ge-Sn alloy stable at room temperature. Moreover, a linear interpolation between the electronic band structures of crystalline Ge and α-Sn predicts a semiconducting behavior for $x \leqslant 0.6$, higher metallic concentrations giving a semimetal structure.[13] Thus, in principle, it is possible to prepare amorphous Ge-Sn films with band gaps varying between 0 and nearly 1 eV. Band-gap variations within this range can also be obtained with Si-Sn alloys, although the crystallization temperatures, the problem of the metal segregation and the composition versus band-gap relationship are different than those referring to Ge-Sn alloys. It is worth remembering, however, that the differences in atom size and in the electronic configuration are smaller between Ge and Sn. As a consequence, it is resonable to expect that narrow-band-gap *a*-Ge:Sn films would be much less defective and would have much better electronic properties than *a*-Si:Sn layers.

The deposition temperature and the hydrogen partial pressure in the reaction chamber are fundamental parameters in relation to transport properties. It is by now well accepted that raising the substrate temperature during deposition or annealing the samples under the crystallization temperature are effective methods to remove electronic states in the pseudogap, eliminating voids and enhancing the full coordination of the network. This process alone does not generally produce an electronic quality amorphous semiconductor which can only be obtained with the use of hydrogen atoms which passivate dangling bonds. The hydrogenation process of tetrahedrally coordinated amorphous semiconductors normally reduces the room-temperature conductivity by orders of magnitude (see Fig. 4).

With these ideas in mind and looking for a narrow-band-gap amorphous semiconductor of good electronic quality, a deposition temperature of 180 °C was chosen for the Ge-Sn alloys. According to the crystallization studies on unhydrogenated *a*-Ge:Sn films referred to above, the maximum tin concentration allowed in the network at this temperature is around 40 at. %. Reference 12 indicates that at this temperature larger tin contents would produce an alloyed polycrystalline material and metal segregation.

Referring to the samples of the present study, we note that only some of those having the largest tin content present metallic segregation. The situation is depicted in Table III, which clearly indicates the influence of the *c*-Si substrate and of the hydrogenation in the enhancement of the segregation

TABLE III. Metal segregation in a-Ge:Sn films sputtered at 180 °C. The influence of hydrogen and of the c-Si substrate in the process is evidenced.

Sample No.	Tin content (at. %)	H_2	Metal segregation	
			Glass subs.	c-Si subs.
07	21	No	No	No
09	27	No	No	Yes
08	···	Yes	No	Yes
10	···	Yes	Yes	Yes

process. In the unhydrogenated sample No. 07 no metallic segregation was detected, while for the same tin/germanium ratio, the presence of hydrogen induces tin segregation on samples of series No. 08 deposited onto c-Si substrates. Sample No. 09 (unhydrogenated) deposited on glass does not indicate any metallic tin at the surface, neither by scanning electron microscopy (SEM) inspection nor by ESCA. On the contrary, the presence of metallic tin on the surface of the film grown onto c-Si was detected by visual inspection. In Fig. 6 a SEM picture of sample No. 09 deposited onto c-Si is shown. The figure also shows x-ray diffraction measurements on the same sample, the spectrum giving the characteristic features of β-Sn. No diffraction peaks corresponding to Ge-Sn crystallites were detected, a result that may be interpreted as being due to either the absence of any crystallization process at a deposition temperature which is well below the T_c reported in Ref. 12 for samples of similar composition, or to the presence of microcrystals not detected by x rays. These results indicate that the substrate may play a role in the process of metal segregation in amorphous Ge-Sn alloys. The increased metal segregation measured in samples grown onto c-Si substrates might also be due to a higher growth temperature resulting from the higher thermal conductivity and the smaller thickness of the silicon substrate.

If hydrogen is added in the reaction chamber while sputtering the target composition of sample No. 09 (sample No. 10), metal segregation occurs in all substrates, the metal

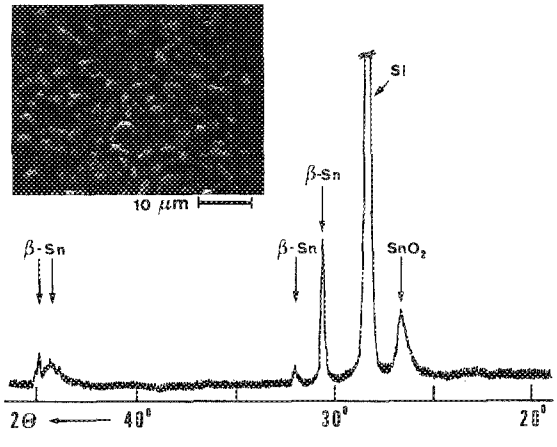

FIG. 6. Scanning electron microscope picture showing the tin particles on the surface of a sample deposited on a c-Si substrate that underwent metallic segregation. The figure also shows the corresponding x-ray diffraction data where the characteristic peaks of the substrate and those of β-Sn and SnO_2 appear.

particles being several micrometers in diameter. The enhancement of metal segregation due to the presence of hydrogen in the reaction chamber has been reported to also occur in a a-$Si_{1-x}Sn_x$:H films prepared by rf sputtering,[14] and explained in terms of different sticking probabilities of Sn to Si atoms at the growing surface, depending on the presence or absence of atomic hydrogen. According to Ref. 14, hydrogen atoms would preferentially attach to Si orbitals, the Si—H bond being stronger than the Sn—H bond. In such a case the incoming Sn atoms are more likely to bond to another Sn on the surface than to a Si atom. The same mechanism, however, cannot explain the present results on Ge-Sn alloys because, on one hand, germanium dangling bonds are less avid for hydrogen atoms than Si dangling bonds[15] and, on the other hand, molecular data on Ge and Sn tetrahydrides[16] indicate that the Ge—H bond strength is similar to the Sn—H one (69 and 73.7 kcal, respectively). Therefore, the preferential attachment mechanism does not suffice to explain the metallic segregation induced by hydrogenation in a-Ge:Sn alloys. At present, an alternative explanation based on the Mössbauer spectra of hydrogenated films and calculations on minimum energy of defective Ge clusters containing Sn atoms is being worked out. The results will be published elsewhere.[17]

B. Transport properties

The results on the dark conductivity of a-Ge and a-Ge:H films shown in Fig. 4 do not differ from those already published in the literature.[9] They indicate the important effects of hydrogenation in the transport properties of tetrahedrally bonded amorphous semiconductors. The cleaning of the electronic states in the pseudogap by the action of H atoms transforms the dc conductivity, dominated by hopping processes between localized states, into an activated type conduction, with carriers in the extended states of the bands. The conductivity and activation energy (0.45 eV) measured in our a-Ge:H samples are in perfect agreement with the model for the density of states in the pseudogap of a-Ge:H proposed by Stutzmann, Stuke, and Dersch.[18]

The results being presented here on the dark conductivity of a-Ge:Sn:H samples suggest that a defect associated to Sn may exist in the lower half of the pseudogap. In effect, the addition of a few percent of tin atoms to the a-Ge host network (sample No. 04) produces very little decrease in the extrapolated optical band gap and a small decrease in the room-temperature (RT) conductivity, which may be associated to a 30-meV increase in the activation energy (E_a). This change in E_a should correspond to a downward shift of the Fermi level produced by a defect center associated to tin atoms. It is tempting to correlate the defect center to a negatively charged Sn pending orbital. In unhydrogenated samples, however, Mössbauer spectra show that up to a value of around 10^{18} cm^{-3} no defect structures exist in tin sites, all Sn atoms being bonded in a covalent tetrahedral configuration.[6] The absence of any Sn-H absorption band in the infrared spectra of a-Ge:Sn:H films suggests that this situation should also prevail in hydrogenated samples. The presence of hydrogen, however, may influence the bonding configura-

tion and the structure of defects around tin sites, as indicated by Mössbauer spectroscopy.[19] Preliminary analyses that take into consideration all these data and the calculations referred to above indicate that an electronic level produced by a different bonding configuration of the tin atom may be at the origin of the downward shift of the Fermi level in hydrogenated samples.[17]

Referring to hydrogenated samples, Fig. 5 shows two regions in the conductivity versus inverse temperature representation, corresponding to different conduction mechanisms. At high temperatures an activated conductivity region appears, the activation energy of which decreases monotonically as the tin content in the network increases. In the high-temperature regime E_a closely follows the optical band-gap narrowing produced by the addition of tin. In this temperature range the overall resistivity reduction with increasing Sn is caused by the activation of carriers across a Fermi-level conduction-band reduced gap. Below this activated region, Fig. 5 shows a nonlinear dependence of conductivity on inverse temperature, an indication of an increased tunneling between an increased density of electronic states at the Fermi level. The analysis of Figs. 4 and 5 also indicates that the transition temperature between activated and mixed conductivity also increases with x, an indication that the electronic states appearing in the pseudogap are produced by tin atoms. Then, it appears that hydrogen becomes a less effective passivating agent as the tin concentration in the alloy raises. An open question is whether this experimental finding is only the consequence of the preparation method or deposition conditions.

In the case of unhydrogenated material, the addition of Sn in any proportion increases the density of defects through which the carriers move and the dc conductivity increases at all temperatures. These results on a-Ge:Sn samples agree well with those of Conell, Temkin, and Paul,[20] who found that the resistivity of their unhydrogenated samples, at temperatures lower than 300 K, decreased monotonically as the tin content was augmented.

Finally, it should be mentioned that under AM1 conditions no photoconductivity was detected in any of the alloyed samples. Under the same irradiation conditions a-Ge:H films of the 02 series possess some photoconductivity, estimated to be of the order of 20% at room temperature. If Sn is added to the Ge network, however, the effect disappears, an indication that the density of electronic states in the pseudogap becomes exceedingly important.

C. Optical properties: The fundamental absorption edge

The electronic band structure of crystalline semiconductors having the diamond and zinc-blende structure may constitute an appropriate starting point of any speculation on the band-gap variations of tetrahedrally bonded amorphous semiconductor alloys, which are known to retain the gross features of the electronic band structure of their crystalline counterparts. A linear interpolation between the electronic band structures of crystalline Ge and α-Sn (Ref. 13) gives, for the alloy, a band-gap variation with a composition of

$$\frac{dE_g}{d\,[\mathrm{Sn}]} = -12 \text{ meV/at. \% Sn.}$$

The above expression predicts a zero-band-gap alloy for a tin content of nearly 66 at. % (see Fig. 7). This linear interpolation is a crude assumption but should roughly reflect the band-gap variation of actual compounds. Temkin *et al.*[5] succeeded in the preparation of amorphous Ge-Sn alloys of composition up to 50-at. % tin. These authors performed ellipsometric and infrared transmission measurements and found a systematic change of the band structure going in the direction of the theoretical predictions, although no figures for band-gap variations with composition were given.

Sato, Yamaguchi, and Ozaki[21] studied the transport properties of amorphous Ge-Sn films prepared by vacuum evaporation. The pseudogap of the films was deduced from dc conductivity measurements for samples containing between 10- and 20-at. % tin. These results are also displayed in Fig. 7, where the linearly interpolated band gap is represented as a function of composition. Figure 7 also shows the extrapolated band gaps of Fig. 1 and Table II. Let us remember that we are considering unhydrogenated samples only.

The band-gap values determined in Ref. 21 do not correspond to either the theoretical predictions or to the experimental determinations of the present paper. Moreover, the optical band gaps extrapolated from the intrinsic absorption region of the samples of the present work confirm the trends and values of the theoretical interpolation between the band structures of c-Ge and α-Sn.

D. Infrared absorption

Although the vibrational properties of a-Ge:H have not been as extensively studied as those of a-Si:H, there is general agreement on the gross features of their main absorptions bands. The interpretation parallels that for a-Si:H.[7] The stretching modes show two components: the 1970-cm^{-1} component is due to $Ge\text{-}H_2$ groupings and to Ge-H inside large cavities while the 1895-cm^{-1} component corresponds to Ge-H in a cavity of the size of a monovacancy. The wagging-rolling mode appears at 565 cm^{-1}, the strength of which has been shown to be proportional to the hydrogen concentration in the material.[22] The spectra do not show any absorption around 800 cm^{-1}, an indication of the absence of polygermane $(GeH_2)_n$.[22,23] As pointed out above, no in-

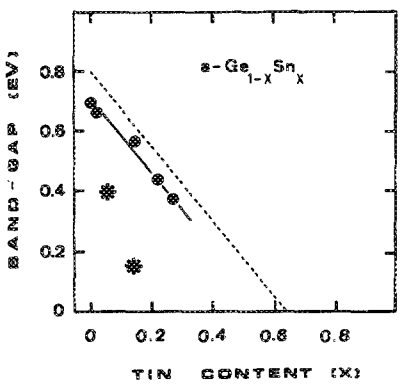

FIG. 7. Band-gap variation of Ge-Sn alloys as a function of composition. The dotted line gives the forbidden band resulting from a linear interpolation between the electronic band structures of c-Ge and β-Sn. The filled stars are the values deduced from conductivity measurements by Sato *et al.*[21] The filled circles correspond to the extrapolated optical gaps of the present work.

frared absorption bands corresponding to the Sn-H stretching modes (which should occur at frequencies below those associated to Ge-H) appear in the transmission spectra of hydrogenated Ge-Sn alloys. The Sn-H wagging vibrations, as well as the infrared absorption band of the Sn—O bonds, are expected to occur within the range of the vibrational frequencies of the host Ge network. It was assumed then that all the hydrogen was bonded to Ge atoms, its concentration being

$$N_H = A_w \int_{\text{wagg}} \omega^{-1}\alpha(\omega)d\omega,$$

where $A_w = 1.1\times10^{19}\ \text{cm}^{-2}$ and $\alpha(\omega)$ is the absorption coefficient of the wagging mode at 565 cm^{-1}. A small shift on the peak value of the infrared absorption bands was measured in the alloys. For example, in sample No. 06 the maximum absorption in the wagging mode occurs at 550 cm^{-1}. The same type of shifts appears in the stretching mode absorptions. This fact simply reflects the different bonding environment provided by the alloyed network to the germanium—hydrogen bonds. The shifts of the peaks calculated, taking into account the Ge and Sn respective masses and their relative concentration in the samples, are in excellent agreement with the measured values. The absence of any absorption at 0.09 eV in our samples was taken as an indication that they were not oxygen contaminated.

V. CONCLUSIONS

This paper provides some new features concerning the semiconductor properties of amorphous Ge-Sn alloys. The use of hydrogenation to passivate defect states of the material is reported for the first time. The preparation conditions leading to low-band-gap amorphous semiconductors are described and the bonding configuration of both elements analyzed. We also reported for the first time on the dependence of the optical band gap as a function of material composition, as well as the limits of tin incorporation to the *a*-Ge network under the reported deposition conditions. The main findings of the work are as follows:

(1) The incorporation of Sn atoms into the *a*-Ge network narrows the band gap at a rate of approximately 12-meV/at. % tin. Conversely, and in a way similar to *a*-Si:H and *a*-Ge:H, the addition of hydrogen widens the optical band gap. A concomitant Ge defect passivation mechanism is found to occur in the samples.

(2) The hydrogenated samples show an activated type dark conductivity, the value of the activation energy depending on the tin content as well as on the hydrogen content. The α-Ge:Sn samples present, on the contrary, a dark conductivity versus temperature behavior typical of electronic conduction through localized states in the pseudogap.

(3) No measurable photoconductivity under AM1 conditions was found in hydrogenated samples containing Sn.

(4) Depending on the deposition temperature, metallic segregation may occur. At 180 °C substrate temperature the segregation mechanism begins for tin concentrations of around 20 at. %. The process proved to also depend on the nature of the substrate and is, in all cases, enhanced by the presence of hydrogen in the reaction chamber.

(5) Infrared transmission spectra of alloyed samples indicate that hydrogen atoms bond only to Ge orbitals. No Sn-H vibrations were detected in the 400–4000-cm^{-1} range. This experimental finding is analyzed in terms of Mössbauer spectra and theoretical calculations.

ACKNOWLEDGMENTS

The authors are indebted to the colleagues of the Laboratory of Photovoltaic Conversion, Institute of Physics, Unicamp, for fruitful discussions. They specially acknowledge Professor R. A. Barrio, UNAM, Mexico, for critical reading of the manuscript. They also thank Professor I. Torriani for x-ray diffraction data, Professor R. Landers for Auger electron spectra, Professor S. C. Castro for ESCA measurements, and Professor C. Ribeiro for scanning electron microscopy and electron-beam microanalysis studies. This research was partially supported by the Fundação de Amparo à Pesquisa do Estado de São Paulo (FAPESP), the Conselho Nacional de Desenvolvimento Cientifico e Tecnologico (CNPq), and the Universidade Estadual de Campinas, Fundo de Apoio a Pesquisa, Brazil.

[1] D. Adler, Kinam **4**, Serie C, Mexico City, 225 (1982).
[2] R. K. Willardson and A. C. Beer, Eds., *Hydrogenated Amorphous Silicon*, Vol. 21 (A–D) of *Semiconductors and Semimetal Series* (Academic, Orlando, FL, 1984).
[3] K. Nozawa, Y. Yamaguchi, J. Hanna, and I. Shimizu, J. Non-Cryst. Solids **59&60**, 533 (1983).
[4] Y. Kuwano, M. Ohnishi, H. Nishiwaki, S. Tsuda, T. Fukatsu, Y. Nakashima, and H. Tarui, in *Proceedings of the 16th IEEE Photovoltaic Specialists Conference* (IEEE, New York, 1982), p. 1338.
[5] R. J. Temkin, G. A. N. Connell, and W. Paul, Solid State Commun. **11**, 1591 (1972).
[6] I. Chambouleyron, F. C. Marques, J. P. Souza, and I. J. R. Baumvol, J. Appl. Phys., **63**, 5596 (1988).
[7] See, for example, the review by M. Cardona, Phys. Status Solidi B **118**, 463 (1983).
[8] G. A. N. Connell and J. R. Pawlik, Phys. Rev. B **13**, 787 (1976).
[9] A. J. Lewis, Phys. Rev. B **14**, 658 (1976).
[10] F. A. Trumbore, J. Electrochem. Soc. **103**, 597 (1956).
[11] V. I. Lisichenko, N. N. Petrichenko, and A. A. Yakumin, Sov. Phys. Solid State **18**, 183 (1976).
[12] R. J. Temkin and W. Paul, in *Amorphous and Liquid Semiconductors*, edited by J. Stuke and W. Brenig (Taylor and Francis, London, 1974), p. 1193.
[13] See, for example, the electronic band structures of *c*-Ge and α-Sn in M. L. Cohen and T. K. Bergtresser, Phys. Rev. **141**, 789 (1966).
[14] D. L. Williamson and S. K. Deb, J. Appl. Phys. **54**, 2588 (1983).
[15] W. Paul, D. K. Paul, B. von Roedern, J. Blake, and S. Oguz, Phys. Rev. Lett. **46**, 1016 (1981).
[16] E. G. Rochow and E. W. Abel, *The Chemistry of Ge, Sn, and Pb*, Vol. 14 of *Texts in Inorganic Chemistry* (Pergamon, United Kingdom, 1975).
[17] R. A. Barrio and I. Chambouleyron (unpublished).
[18] M. Stutzmann, J. Stuke, and H. Dersch, Phys. Status Solidi B **115**, 141 (1983).
[19] I. Chambouleyron, F. C. Marques, P. H. Dionisio, and I. J. R. Baumvol (unpublished).
[20] G. A. N. Connell, R. J. Temkin, and W. Paul, in *Amorphous and Liquid Semiconductors*, edited by J. Stuke and W. Brenig (Taylor and Francis, London, 1974), p. 1201.
[21] S. Sato, N. Yamaguchi, and H. Ozaki, J. Phys. Soc. Jpn. **33**, 1497 (1972).
[22] C. J. Fang, K. J. Grunz, L. Ley, M. Cardona, F. J. Demond, G. Muller, and S. Kalbitzer, J. Non-Cryst. Solids **35 & 36**, 255 (1980).
[23] G. Lucovsky, S. S. Chao, J. Yang, J. E. Tyler, R. C. Ross, and W. Czubatyj, Phys. Rev. B **31**, 2190 (1985).